[Original Article]

Autophagy is involved in the sclerotic phase of systemic sclerosis

Tatsuhiko Mori[1], Naoki Tamura[2], Satoshi Waguri[2] and Toshiyuki Yamamoto[1]

[1]*Department of Dermatology, School of Medicine, Fukushima Medical University, Fukushima, Japan,*
[2]*Department of Anatomy and Histology, School of Medicine, Fukushima Medical University, Fukushima, Japan*

Abstract Autophagy is an essential intracellular self-degradation system, and is known to maintain the homeostatic balance between the synthesis, degradation, and recycling of cellular proteins and organelles. Recent studies have suggested a possible role of autophagy in systemic sclerosis (SSc) ; however, differences in autophagy among pathological phases of SSc have not yet been examined. Therefore, in the current study we investigated the expression pattern of an autophagosome marker protein, microtubule-associated protein 1 light chain 3 (LC3) in the lesional skin of a murine model and human SSc. In bleomycin-induced mouse scleroderma skin, the number of LC3-positive puncta was significantly higher than that in phosphate buffered salts-injected control skin after 4 weeks of treatment. Such an increase, however, was not observed in the skin after 2 weeks of bleomycin treatment, in which few myofibroblasts were detected. In the sclerotic phase of SSc patients, the number of LC3-positive puncta in the lower dermis was significantly higher than in the upper dermis. It was also significantly higher than in the lower dermis of the control patients. No increase in LC3-positive puncta was observed in the skin from SSc patients in edematous phase, in which myofibroblasts were hardly detected. These results suggest that changes in the autophagic degradation system reflect a skin remodeling process that leads to fibrosis.

Key words : LC3, lysosome, scleroderma, murine model, bleomycin

Introduction

Autophagy is an essential intracellular self-degradation system known to maintain the homeostatic balance between the synthesis, degradation, and recycling of cellular proteins and organelles[1-3]. It is induced by a variety of stress stimuli, such as nutrient starvation and ischemia, and is initiated by the formation of a double membrane structure, called an isolation membrane, which elongates to enclose a portion of the cytoplasm and/or organelles. When the isolation membrane completely closes, it becomes an autophagosome, which further acquires lysosomal enzymes by fusion with lysosomes for degradation of its contents, resulting in a structure called an autolysosome. Microtubule-associated protein 1 light chain 3 (LC3) is an autophagy-related gene (Atg) product, and is known to be a marker of the isolation membranes, autophagosomes, and a fraction of autolysosomes[4-7].

Impairments of autophagy are often associated with various diseases, such as malignant tumors, heart failure and type 2 diabetes mellitus[8-12]. Previous studies have shown that skin specimens from systemic sclerosis (SSc) patients have more intense LC3 immunoreactivity than those from healthy controls[13], whereas another study suggested that SSc fibroblasts show impaired autophagy[14]. Therefore, the involvement of autophagy in SSc has not yet been fully elucidated. In the present study, we focused on the differences in the LC3 expression pattern among different phases of SSc progression, and investigated the involvement of the autophagy system.

Methods

Animal experiment

Specific pathogen-free C57BL/6J male mice (7 weeks old) were purchased from CHARLES RIVER LABORATORIES JAPAN, Inc. (Kanagawa, Japan), and were housed in a controlled environment (21-24°C, 60% humidity, 12-h light/dark cycle). The mice were fed ad libitum (two mice) or starved for 24 hours (three mice) before being anesthetized by intraperitoneal injection of 25 mg/kg pentobarbital sodium (Kyoritsu Seiyaku Corporation, Tokyo, Japan). They were then perfused via the heart, first with Ringer's solution and then with a fixative solution of 4% paraformaldehyde and 4% sucrose in phosphate buffer (pH 7.4). The livers were excised and processed for paraffin embedding.

To generate a mouse model for SSc, specific pathogen-free C3H/HeJ female mice (6 weeks old) were used, as reported previously[15,16]. The mice were purchased from CLEA Japan, Inc. (Tokyo, Japan), and were housed in a controlled environment (21-24°C, 60% humidity, 12-h light/dark cycle), and fed ad libitum. The mice were intradermally injected with 50 μg bleomycin (BLM) (Nippon Kayaku Co. Ltd., Tokyo, Japan) in phosphate-buffered saline (PBS) or PBS alone into the backs once daily for 5 days per week for 2 or 4 weeks. Five mice were used for each group. The mice were anesthetized by inhalation of 2.5% isoflurane (Mylan Inc., Tokyo, Japan), and skin samples were biopsied from the injected site. These samples were fixed in 10% formalin neutral buffer solution (Wako Pure Chemical Corporation, Osaka, Japan) overnight and embedded in paraffin. All experimental procedures were approved by the Animal Care and Use Committee of Fukushima Medical University (approval numbers 27016 and 28016).

Human samples

The SSc patients were diagnosed according to the SSc diagnostic criteria outlined by the Japanese Dermatological Association. The patients included were five edematous phase SSc (E-SSc) patients, and five sclerotic phase SSc (S-SSc) patients, whose clinical characteristics are shown in Table 2. Skin samples were biopsied from each patient's forearm. Control skins were obtained from the edge of the resected benign tumors, such as epidermal cyst and verruca vulgaris, on the forearms of 5 healthy patients (Table 2). All human skin samples were fixed in 10% formalin neutral buffer solution (Wako

Pure Chemical Corporation) overnight and embedded in paraffin. All experimental procedures were approved by the Ethics Committee of Fukushima Medical University (approval number 2472).

Immunohistological analyses

The paraffin-embedded samples were sectioned at 3 μm thickness, then deparaffinized and rehydrated. For evaluation of skin fibrosis, the sections were stained with hematoxylin and eosin (HE), or by immunohistochemistry using anti-α smooth muscle actin (αSMA) antibody. As demonstrated in a previous study by Kissin *et al.*, αSMA-positive myofibroblasts increase in the skin lesion of SSc patients[17]. For the immunohistochemistry, the sections were incubated with 3% hydrogen peroxide in methanol, and then blocked with 10% normal goat serum (Nichirei Biosciences Inc. [Tokyo, Japan], 426042). Next, the sections were incubated with anti-αSMA antibody (Abcam plc [Cambridge, UK], ab7817) at a dilution of 1 : 100 in an antibody diluent (Roche Diagnostics K.K. [Basel, Switzerland], 251-018) for 1.5 h at room temperature, followed by incubation with a mixture of peroxidase-conjugated goat anti-mouse and anti-rabbit IgGs (Nichirei Biosciences Inc., 424151, Simple Stain MAX PO [MULTI]) for 30 min at room temperature. Color development was performed using a DAB substrate kit (Nichirei Biosciences Inc., 425011). The sections were then counterstained with hematoxylin. For immunohistofluorescence microscopy analysis, the sections were blocked with 5% normal donkey serum (Jackson ImmunoResearch Laboratories Inc. [PA, USA], 017-000-121), and incubated overnight with rabbit monoclonal antibody against LC3A (Abcam plc, ab52768 ; at a dilution of 1 : 400 in blocking solution), at 4°C. Donkey anti-rabbit IgG conjugated with a fluorescent dye, Alexa Fluor 488 (Jackson ImmunoResearch Laboratories Inc., 711-545-152) or Alexa Fluor 594 (Jackson ImmunoResearch Laboratories Inc., 715-585-150), was used as a secondary antibody. Hoechst 33342 (Thermo Fisher Scientific, Inc. [MA, USA], H3570) was used for nuclear staining. The sections were washed with PBS containing 0.1% Tween-20. They were then viewed with a laser scanning confocal microscope, FV1000 (Olympus, Tokyo, Japan). For quantification, five regions of interest (ROI) with a size of 105 × 105 μm were randomly captured in the dermis of the mice, and in the upper and lower dermis of the patients. LC3-positive puncta with a diameter of 0.3-1 μm were counted, then further divided by the number of nuclei in the ROI. The

signals of LC3 and nuclei in blood vessels, hair follicles, nerves, and arrector pili muscles were excluded from this measurement.

Statistical analysis

All data are expressed as a box-and-whisker plot, and analyzed using EZR software (version 1.35 ; Saitama Medical Center, Jichi Medical University, Japan)[18]. Statistical differences were evaluated by the Mann-Whitney U test or the Steel Dwass test, and values of $P < 0.05$ were considered statistically significant.

Results

LC3-positive puncta in BLM-treated mouse skin

On observing the HE-stained sections, dermal fibrosis was apparent in the 4-week BLM-treated mice when compared to the PBS-treated ones, although the fibrosis was less evident in the 2-week BLM-treated mice (Figure 1A). More αSMA-positive myofibroblasts were detected in the dermis of the 4-week BLM-treated than the PBS-treated mice. Additionally, these myofibroblasts were hardly detected in the 2-week BLM-treated mice (Figure 1B).

We next examined LC3 distribution by immunohistofluorescence microscopy. The anti-LC3 antibody used in this study was confirmed to detect endogenous mouse LC3, because LC3-positive puncta increased in the starved mouse livers compared to those in the fed mouse livers (Figure 1C).

Similar puncta were observed in the dermis, most markedly in the 4-week BLM-treated mice (Table 1, Figure 1D, 1E). Quantitative analysis revealed that the number of LC3-positive puncta was significantly higher in the 4-week BLM-treated mice (0.117±0.046) than in the 4-week PBS-treated mice (0.063±0.036 ; $P = 0.032$ in Mann-Whitney U test, $n = 5$; Figure 1F). There was no significant difference between the 2-week BLM- and PBS-treated mice. Although the median number of LC3-positive puncta in the 4-week BLM-treated mice was higher than that in the 2-week BLM-treated mice, the difference was not statistically significant.

LC3-positive puncta in SSc patients

HE-analysis revealed that dermal fibrosis in S-SSc was more severe than that in E-SSc (Figure 2A). Regional differences were also evaluated in this analysis, because previous studies indicated that

the lower dermis of SSc patients contains increased collagen bundles, fibronectin, and myofibroblasts[17,19,20]. The current study also showed that collagen bundles in the lower dermis were denser than in the upper dermis in both E-SSc and S-SSc samples (Figure 2A). As shown in Figure 2B, numerous αSMA-positive myofibroblasts were observed in the lower dermis of S-SSc samples, but they were hardly detected in the upper dermis of those samples. Neither were they detected in either the lower or upper dermis of the E-SSc samples. As for LC3-positive puncta, remarkable signals were observed in the lower dermis of the S-SSc samples (Figure 2E), whereas they were weak in the dermis of the controls, E-SSc samples, and the upper dermis of the S-SSc samples (Figures 2C-E). There were more LC3-positive puncta in the lower dermis of the S-SSc samples (0.854 ± 0.310) than in the lower dermis of the controls (0.141 ± 0.054 ; $P = 0.043$ in Steel-Dwass test ; Figure 2F) or the upper dermis of S-SSc samples (0.264 ± 0.140 ; $P = 0.032$ in Mann-Whitney U test ; Figure 2F). On the other hand, there was no significant difference between the upper dermis of the S-SSc samples, and the E-SSc samples (0.135 ± 0.067) or controls (0.069 ± 0.060).

Discussion

The current study demonstrated a high number of LC3-positive puncta in the lesional dermis of BLM-treated mice and S-SSc patients compared to controls. These results are consistent with those of previous studies demonstrating that the tissue sections of SSc patients showed more intense LC3 immunoreactivity than those taken from healthy controls[13]. However, we further advanced this understanding by demonstrating the differences in regions and degrees of fibrosis. We showed that the number of LC3-positive puncta was significantly high in severely fibrotic dermis, such as in the lower dermis of the S-SSc samples and murine dermis treated with BLM for 4 weeks. In contrast, no difference was observed in mildly fibrotic dermis, such as the upper dermis of the S-SSc samples, the dermis of the E-SSc samples and the murine dermis treated with BLM for 2 weeks. Therefore, these results suggest that the autophagy-lysosomal pathway is closely correlated with the sclerotic phase, where fibrosis proceeds, and that the involvement of early immunological changes may be unlikely.

Given that LC3 is localized to the isolation membrane, autophagosomes, and a fraction of autol-
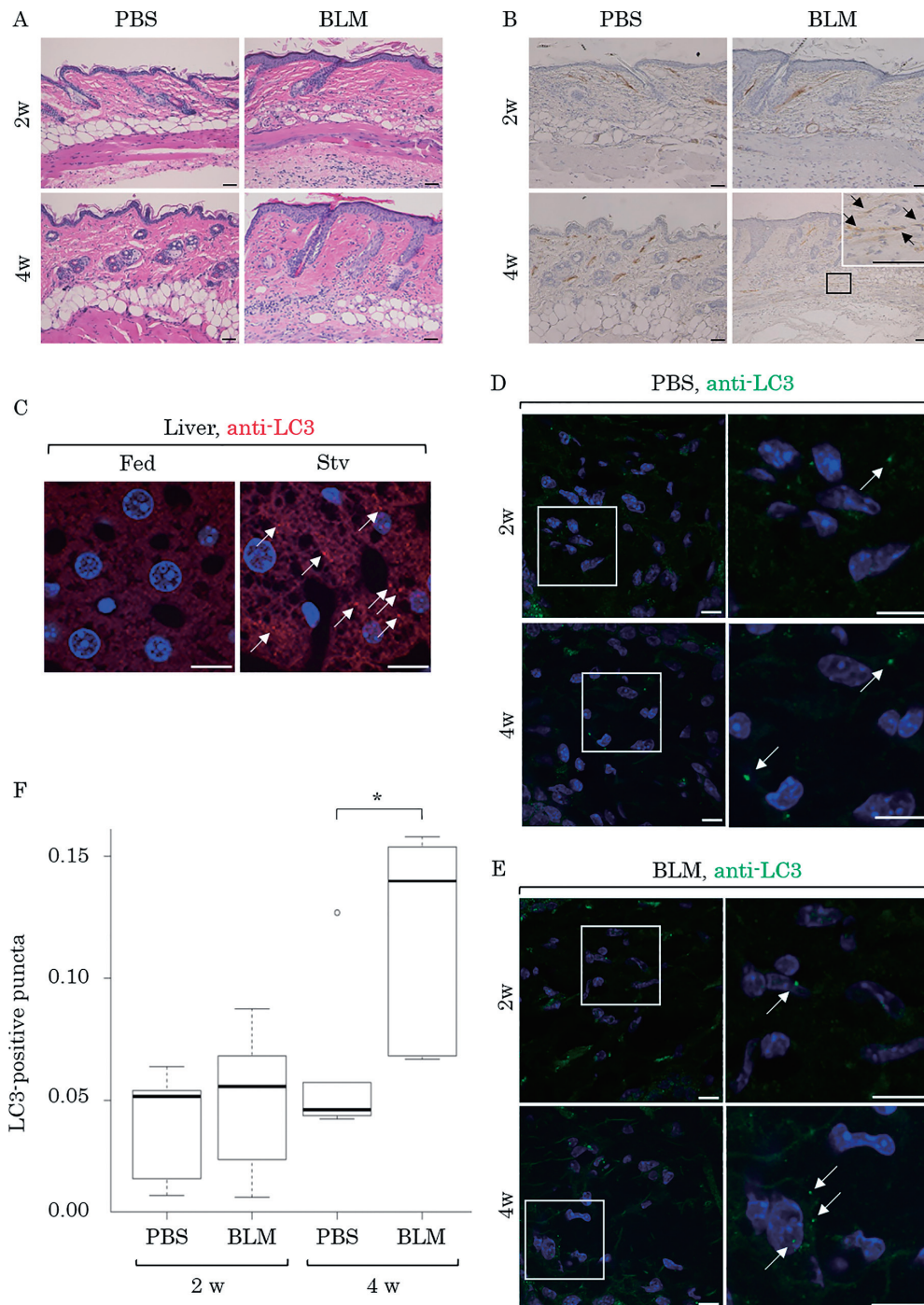
Fig. 1.   LC3-positive puncta in the skin of BLM-treated mice

Mice were treated with PBS or BLM for 2 weeks (2w) or 4 weeks (4w).   The skin samples were examined by HE staining (A) or immunohistochemistry for αSMA (B).   The boxed region is magnified and shown in the inset.   The arrows indicate αSMA-positive myofibroblasts.   Scale bars, 50 μm.   Mouse livers with 24-hour starvation (Stv) or without (Fed) were processed for immunohistofluorescence microscopy analysis using anti-LC3 antibody (anti-LC3 ; red) followed by Alexa Fluor 594-conjugated secondary antibody (C).   The nuclei were stained with Hoechst 33342 (blue).   Scale bar, 10 μm.   The skin samples from the mice treated with PBS (D) or BLM (E) for 2 weeks (2w) or 4 weeks (4w) were immunolabeled using anti-LC3 antibody (anti-LC3 ; green) followed by Alexa Fluor 488-conjugated secondary antibody.   The nuclei were stained with Hoechst 33342 (blue).   The boxed regions are magnified and shown on the right.   The arrows indicate LC3-positive puncta observed in the dermis.   Scale bars, 10 μm.   LC3-positive puncta (number/nuclei) in ROIs were measured and are expressed as a box-and-whisker plot in F.   The boxes indicate the upper and lower interquartile range (IQR), the lines within the boxes indicate the median, the whiskers indicate the minimum and maximum IQR, and the dot indicates the outlier.   * : significant difference ($P < 0.05$ in Mann-Whitney U test).

Table 1. The number of LC3-positive puncta in the dermis of the mice

Mouse type	LC3-positive puncta per cell
PBS 2 week	0.064
	0.018
	0.054
	0.011
	0.051
BLM 2 week	0.056
	0.088
	0.01
	0.068
	0.026
PBS 4 week	0.127
	0.046
	0.042
	0.044
	0.057
BLM 4 week	0.158
	0.154
	0.068
	0.14
	0.067

Some mechanisms could be considered to link such fibrosis with the increase of LC3-positive puncta. Transforming growth factor-beta (TGF-beta) is known to play an important role during fibrosis[28]. Its signaling pathway has been reported to increase the mRNA expression of several Atgs, such as Beclin 1, Atg5, Atg7, death-associated protein kinase, and LC3 through both Smad-dependent and independent pathways[29-31]. Therefore, the TGF-beta/Smad pathway may cause the increase of LC3-positive puncta. Moreover, from a histological aspect, severe fibrosis might cause a nutritional insufficiency for fibroblasts in the dermis, which may lead to starvation-induced autophagy or somehow suppress lysosomal degradation. It is also possible that cellular differentiation into myofibroblasts involves autophagy-lysosomal degradation[32].

In conclusion, the findings of the current study suggest that the autophagy-lysosomal pathway is involved in the sclerotic phase of SSc. There are several limitations, such as small sample size, and lack of association with disease duration and skin sclerosis score in human SSc. Future studies focusing on the relationship between the histological fibrosis and autophagy-lysosomal system would be required to clarify the underling mechanisms of the disease progression of SSc.
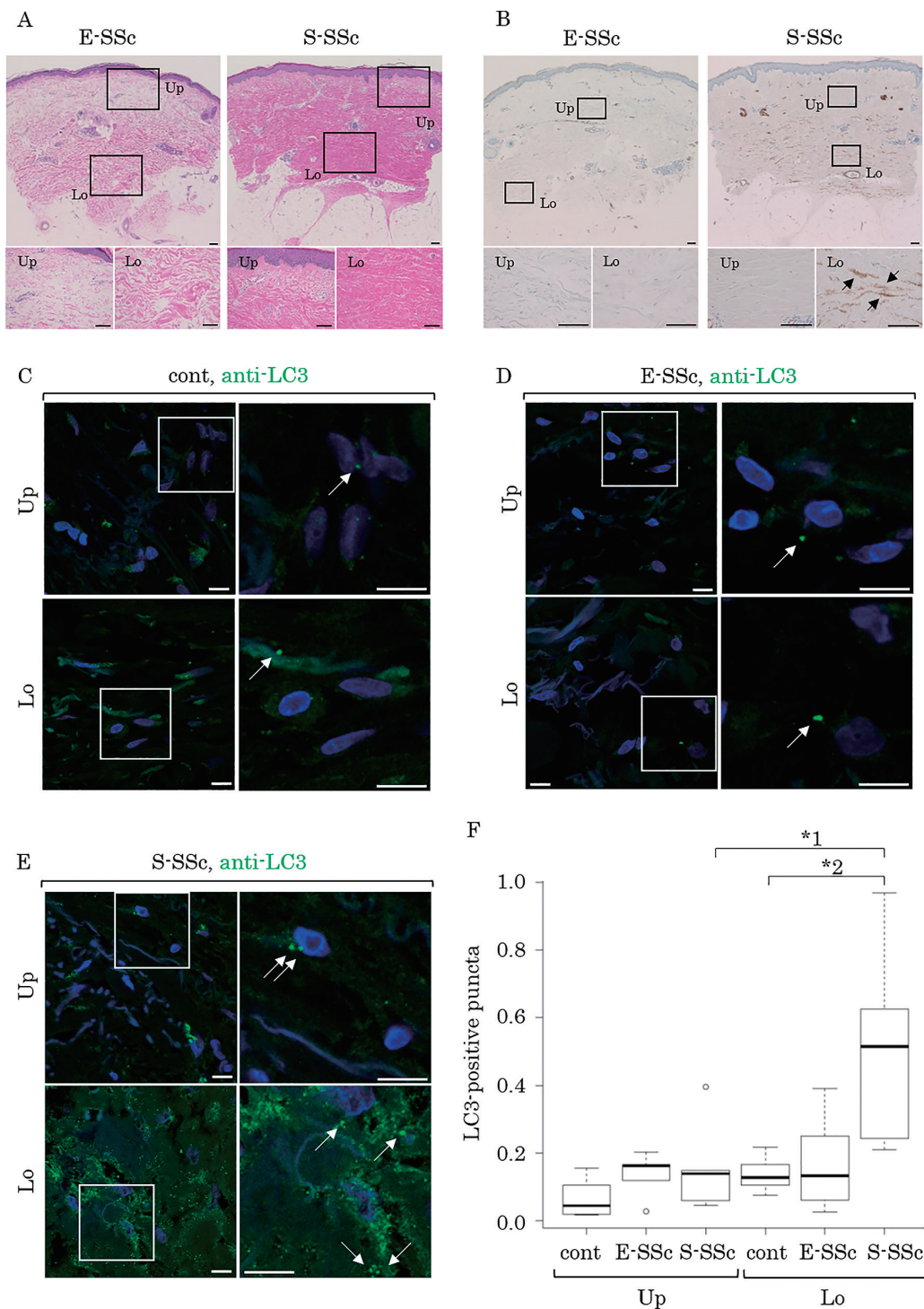
Acknowledgments

ysosomes[5-7], the increase in the number of intracellular LC3-positive puncta reflects autophagy activation and/or the suppression of lysosomal degradation of LC3. Therefore, it remains controversial as to whether autophagy is really induced or not in SSc skin. It has previously been reported that autophagy is activated in BLM-treated mouse lung[21-23], which is consistent with the present results of BLM-induced LC3-positive puncta in the mouse skin. Furthermore, previous studies that conducted knockdown experiments of core Atg genes, Atg5 or Atg7, as well as pharmacological experiments using autophagy inhibitors (chloroquine and 3-methyladenine), reported positive roles of autophagy in liver fibrosis[24] and the transdifferentiation of cardiac myofibroblasts[25]. Hydroxychloroquine, also an autophagy inhibitor, reduced the metabolic activity and suppressed cell proliferation of human fibroblasts[26]. However, it has been reported that SSc fibroblasts showed impaired autophagy[14], which might promote myofibroblast differentiation in idiopathic pulmonary fibrosis patients[27]. These reports suggest that the suppression of autophagy occurs in SSc as well as other fibrotic conditions.

Fig. 2.   LC3-positive puncta in the skin of SSc patients
E-SSc and S-SSc specimens were examined by HE-staining (A) and immunohistochemistry for αSMA (B).   The upper (Up) and lower (Lo) regions of the dermis (boxed) are magnified and shown on the bottom half of the image.   The arrows in the lower dermis of the S-SSc indicate αSMA-positive myofibroblasts.   Scale bars, 100 μm.   The control (C), E-SSc (D) and S-SSc (E) specimens were examined by immunostaining for LC3 (anti-LC3 ; green) followed by Alexa Fluor 488-conjugated secondary antibody.   The upper (Up) and lower (Lo) regions of the dermis are shown.   The boxed regions are magnified and shown on the right.   The arrows indicate LC3-positive puncta observed in the dermis.   Scale bars, 10 μm.   LC3-positive puncta (number/nuclei) in ROIs were measured and are expressed as a box-and-whisker plot in F.   The boxes indicate the upper and lower IQR, the lines within the boxes indicate the median, the whiskers indicate the minimum and maximum IQR, and the dots indicate the outliers.   "*1" and "*2" indicate significant difference ($P < 0.05$) according to the Mann-Whitney U test and Steel Dwass test, respectively.

Table 2. Clinical characteristics of SSc patients and controls

SSc type	Age	Sex	Skin symptoms other than skin fibrosis	Autoantibody	Organ involvement	LC3-positive puncta per cell	
						upper dermis	lower dermis
E-SSc	55	F	Raynaud	centromere	–	0.12	0.026
	63	F	Raynaud, nail fold bleeding	–	–	0.164	0.25
	63	F	–	U1-RNP	interstitial lung disease	0.203	0.39
	68	F	nail fold bleeding	centromere	–	0.027	0.133
	79	M	–	centromere	interstitial lung disease, primary biliary cirrhosis	0.163	0.063
S-SSc	7	F	nail fold bleeding, digital ulcer	Scl-70	interstitial lung disease, arthritis, myositis	0.047	0.211
	27	F	Raynaud, nail fold bleeding	U1-RNP	–	0.061	0.243
	47	F	Raynaud, leg livedo	–	interstitial lung disease	0.149	0.625
	51	F	Raynaud, nail fold bleeding	centromere	arthritis	0.14	0.968
	63	M	Raynaud, digital ulcer	–	interstitial lung disease, aortic regurgitation, left ventricular hypertrophy	0.396	0.515
Control	33	F				0.019	0.217
	57	F				0.045	0.119
	64	F				0.105	0.075
	69	F				0.156	0.128
	84	F				0.018	0.167

References

1. de Duve C. The lysosome turns fifty. Nat Cell Biol, **7** : 847-849, 2005.
2. Klionsky DJ. Autophagy : from phenomenology to molecular understanding in less than a decade. Nat Rev Mol Cell Biol, **8** : 931-937, 2007.
3. Duszenko M, Ginger ML, Brennand A, *et al.* Autophagy in protists. Autophagy, **7** : 127-158, 2011.
4. Mizushima N, Yoshimori T, Ohsumi Y. The role of Atg proteins in autophagosome formation. Annu Rev Cell Dev Biol, **27** : 107-132, 2011.
5. Mizushima N, Yoshimori T, Levine B. Methods in mammalian autophagy research. Cell, **140** : 313-326, 2010.
6. Mizushima N, Yamamoto A, Matsui M, Yoshimori T, Ohsumi Y. In vivo analysis of autophagy in response to nutrient starvation using transgenic mice expressing a fluorescent autophagosome marker. Mol Biol Cell, **15** : 1101-1111, 2004.
7. Kabeya Y, Mizushima N, Ueno T, *et al.* LC3, a mammalian homologue of yeast Apg8p, is localized in autophagosome membranes after processing. EMBO J, **19** : 5720-5728, 2000.
8. Komatsu M, Waguri S, Chiba T, *et al.* Loss of autophagy in the central nervous system causes neurodegeneration in mice. Nature, **441** : 880-884, 2006.
9. Nixon RA. The role of autophagy in neurodegenerative disease. Nat Med, **19** : 983-997, 2013.
10. Nishida K, Kyoi S, Yamaguchi O, Sadoshima J, Otsu K. The role of autophagy in the heart. Cell Death Differ, **16** : 31-38, 2009.
11. Jung HS, Lee MS. Role of autophagy in diabetes and mitochondria. Ann N Y Acad Sci, **1201** : 79-83, 2010.
12. Mathew R, Karantza-Wadsworth V, White E. Role of autophagy in cancer. Nat Rev Cancer, **7** : 961-967, 2007.
13. Frech T, De Domenico I, Murtaugh MA, *et al.* Autophagy is a key feature in the pathogenesis of systemic sclerosis. Rheumatol Int, **34** : 435-439, 2014.
14. Dumit VI, Küttner V, Käppler J, *et al.* Altered MCM protein levels and autophagic flux in aged and systemic sclerosis dermal fibroblasts. J Invest Dermatol, **134** : 2321-2330, 2014.
15. Yamamoto T, Kuroda M, Nishioka K. Animal model of sclerotic skin. III : Histopathological comparison of bleomycin-induced scleroderma in various mice strains. Arch Dermatol Res, **292** : 535-541, 2000.
16. Yamamoto T, Takagawa S, Katayama I, *et al.* Ani-

mal model of sclerotic skin. I : Local injections of bleomycin induce sclerotic skin mimicking scleroderma. J Invest Dermatol, **112** : 456-462, 1999.

17. Kissin EY, Merkel PA, Lafyatis R. Myofibroblasts and hyalinized collagen as markers of skin disease in systemic sclerosis. Arthritis Rheum, **54** : 3655-3660, 2006.

18. Kanda Y. Investigation of the freely available easy-to-use software 'EZR' for medical statistics. Bone Marrow Transplant, **48** : 452-458, 2013.

19. Cooper SM, Keyser AJ, Beaulieu AD, Ruoslahti E, Nimni ME, Quismorio FP Jr. Increase in fibronectin in the deep dermis of involved skin in progressive systemic sclerosis. Arthritis Rheum, **22** : 983-987, 1979.

20. Ackerman AB, Chongchitnant N, Sanchez J, *et al.* Scleroderma. *In* : Histologic Diagnosis of Inflammatory Skin Diseases second edition. Williams & Wilkins, Baltimore, 706-721, 1997.

21. Mi S, Li Z, Yang HZ, Liu H, *et al.* Blocking IL-17A promotes the resolution of pulmonary inflammation and fibrosis via TGF-beta1-dependent and -independent mechanisms. J Immunol, **187** : 3003-3014, 2011.

22. Cabrera S, Maciel M, Herrera I, *et al.* Essential role for the ATG4B protease and autophagy in bleomycin-induced pulmonary fibrosis. Autophagy, **11** : 670-684, 2015.

23. Yang HZ, Wang JP, Mi S, *et al.* TLR4 activity is required in the resolution of pulmonary inflammation and fibrosis after acute and chronic lung injury. Am J Pathol, **180** : 275-292, 2012.

24. Hernández-Gea V, Ghiassi-Nejad Z, Rozenfeld R, *et al.* Autophagy releases lipid that promotes fibro-

genesis by activated hepatic stellate cells in mice and in human tissues. Gastroenterology, **142** : 938-946, 2012.

25. Gupta SS, Zeglinski MR, Rattan SG, *et al.* Inhibition of autophagy inhibits the conversion of cardiac fibroblasts to cardiac myofibroblasts. Oncotarget, **7** : 78516-78531, 2016.

26. Ramser B, Kokot A, Metze D, *et al.* Hydroxychloroquine Modulates Metabolic Activity and Proliferation and Induces Autophagic Cell Death of Human Dermal Fibroblasts. J Invest Dermatol, **129** : 2419-2426, 2009.

27. Araya J, Kojima J, Takasaka N, *et al.* Insufficient autophagy in idiopathic pulmonary fibrosis. Am J Physiol Lung Cell Mol Physiol, **304** : L56-69, 2013.

28. Varga J, Abraham D. Systemic sclerosis : a prototypic multisystem fibrotic disorder. J Clin Invest, **117** : 557-567, 2007.

29. Ding Y, Kim JK, Kim SI, *et al.* TGF-{beta}1 protects against mesangial cell apoptosis via induction of autophagy. J Biol Chem, **285** : 37909-37919, 2010.

30. Kiyono K, Suzuki HI, Matsuyama H, *et al.* Autophagy is activated by TGF-beta and potentiates TGF-beta-mediated growth inhibition in human hepatocellular carcinoma cells. Cancer Res, **69** : 8844-8852, 2009.

31. He C, Klionsky DJ. Regulation mechanisms and signaling pathways of autophagy. Annu Rev Genet, **43** : 67-93, 2009.

32. Asai E, Yamamoto M, Ueda K, Waguri S. Spatiotemporal alterations of autophagy marker LC3 in rat skin fibroblasts during wound healing process. Fukushima J Med Sci, **64** : 15-22, 2018.